

Supplementary Information

Armored Cobalt-Citrate Framework with Graphene Oxide Exhibiting Improved Thermal Stability and Selectivity for Biogas Decarburization

Yangcan Shen,^{1,2} Ziyin Li,¹ Lihua Wang,¹ Yingxiang Ye,¹ Qing Liu,¹ Xiuling Ma,¹ Qianhou Chen,¹
Zhangjing Zhang^{1,*} and Shengchang Xiang^{1,3,*}

¹ Fujian Provincial Key Laboratory of Polymer Materials, College of Material Sciences and Engineering, Fujian Normal University, 32 Shangsan Road, Fuzhou 350007, China

² State Key Laboratory of Structural Chemistry, Fujian Institute of Research on the Structure of Matter, Chinese Academy of Sciences, Fuzhou, Fujian 350002, PR China

³ College of Life and Environmental Sciences, Minzu University of China, 27 South Zhongguancun Boulevard, Haidian District, Beijing 100081, China

* To whom correspondence should be addressed.

Email addresses: Z.-J. Zhang (zzhang@fjnu.edu.cn) and S.-C. Xiang (scxiang@fjnu.edu.cn)

Contents

Table S1 Summary of the parameters and the enthalpies of gas adsorption on UTSA-16-GO composites at 296 and 273 K obtained from the virial equation.....	S3
Table S2 Adsorption selectivities for equimolar CO ₂ /CH ₄ mixture at 200 kPa and 296 K by IAST on different MOFs	S4
Figure S1 FTIR spectra of as-synthesized GO, UTSA-16 and composites.....	S5
Figure S2 SEM images for the composites.....	S6
Figure S3 TEM images for UTSA-16.....	S6
Figure S4 TEM images for the composites.....	S6
Figure S5 (a) Cumulative pore volume and (b) pore-size distribution for UTSA-16 and its composites.....	S7
Figure S6 The virial graphs for adsorption of CO ₂ on UTSA-16-GO9.5.....	S8
Figure S7 The virial graphs for adsorption of CH ₄ on UTSA-16-GO9.5.....	S8
Figure S8 The virial graphs for adsorption of CO ₂ on UTSA-16-GO19.....	S8
Figure S9 The virial graphs for adsorption of CH ₄ on UTSA-16-GO19.....	S9
Figure S10 The virial graphs for adsorption of CO ₂ on UTSA-16-GO28.5.....	S9
Figure S11 The virial graphs for adsorption of CH ₄ on UTSA-16-GO28.5.....	S9
Figure S12 Comparison of the enthalpies for gas adsorption of CO ₂ , CH ₄ on UTSA-16-GO9.5 from two methods: virial equation (solid) and linear extrapolation (open)	S10
Figure S13 Comparison of the enthalpies for gas adsorption of CO ₂ , CH ₄ on UTSA-16-GO19 from two methods: virial equation (solid) and linear extrapolation (open)	S10
Figure S14 Comparison of the enthalpies for gas adsorption of CO ₂ , CH ₄ on UTSA-16-GO28.5 from two methods: virial equation (solid) and linear extrapolation (open)	S10
Figure S15 The graphs of the Single-site Langmuir-Freundlich equations fit for adsorption of CO ₂ (left) and CH ₄ (right) on UTSA-16-GO9.5 at 296K.....	S11
Figure S16 The graphs of the Single-site Langmuir-Freundlich equations fit for adsorption of CO ₂ (left) and CH ₄ (right) on UTSA-16-GO19 at 296K.....	S11
Figure S17 The graphs of the Single-site Langmuir-Freundlich equations fit for adsorption of CO ₂ (left) and CH ₄ (right) on UTSA-16-GO28.5 at 296K.....	S11
Supplementary References.....	S12

Table S1 | Summary of the parameters and the enthalpies of gas adsorption on UTSA-16-GO composites at 296 and 273 K obtained from the virial equation, as shown in Figures S6~S11.

Sample	adsorbate	T/ K	$A_0/ln(mol g^{-1} Pa^{-1})$	$A_1/g mol^{-1}$	R^2	$\Delta H/kJ mol^{-1}$
UTSA-16-GO9.5	CO ₂	296	-12.780±0.112	-1684.456±27.666	0.998	36.1
		273	-11.544±0.141	-2002.903±41.121	0.998	
	CH ₄	296	-19.471±0.001	-420.455±4.349	0.999	10.9
		273	-19.097±0.001	-324.566±12.874	0.994	
UTSA-16-GO19	CO ₂	296	-12.059±0.092	-1405.067±29.558	0.996	42.1
		273	-10.616±0.119	-1653.615±37.188	0.998	
	CH ₄	296	-19.038±0.002	-296.732±7.023	0.996	11.7
		273	-18.646±3.946E-4	-251.911±1.888	0.999	
UTSA-16-GO28.5	CO ₂	296	-12.021±0.075	-1943.720±56.301	0.994	40.0
		273	-10.650±0.113	-2285.230±70.018	0.996	
	CH ₄	296	-19.176±6.443E-4	-407.189±8.954	0.996	11.4
		273	-18.800±0.002	-402.117±11.438	0.996	

Table S2 | Adsorption selectivities for equimolar CO₂/CH₄ mixture at 200 kPa and 296 K by IAST on different MOFs.

MOFs	T / K	S_{ads} (CO ₂ /CH ₄)	Supplementary References
polyamine incorporated amine-MIL-101 (Cr) (c)	298	931	1
polyamine incorporated amine-MIL-101 (Cr) (b)	298	278	1
UTSA-16-GO19	296	114.4	This work
MgMOF-74	296	105	2
UTSA-16-GO9.5	296	98.7	This work
UTSA-16-GO28.5	296	89.4	This work
[Cd ₂ L1(H ₂ O)] ₂ ·5H ₂ O	298	66	3
UTSA-16	296	29.8	2
polyamine incorporated amine-MIL-101 (Cr) (a)	298	21	1
Fe ₂ (dobdc)	298	20.2	4
UiO-66(Zr)-CO ₂ H	298	19.2	5
MOF-5 (IRMOF-1)	298	15.5	6
UTSA-15a	296	14.2	2
Cu-TDPAT	296	13.8	2
bio-MOF-11	298	~12	7
Cu(bpy-1) ₂ (SiF ₆)	298	~11	8
Zn ₅ (BTA) ₆ (TDA) ₂	296	10.8	2
ZIF-78	296	10.4	2
MIL-101	296	9.6	9
UTSA-72a	293	9.6	10
UTSA-25a	296	9.4	2
UTSA-20a	296	8.3	2
Fe ₂ (O ₂)(dobdc)	298	7.8	4
CuBTC	296	7.4	9
UTSA-33a	296	7.0	2
MIL-53	298	7	11
UTSA-34b	296	5.1	2
MOF-177	298	4.4	6

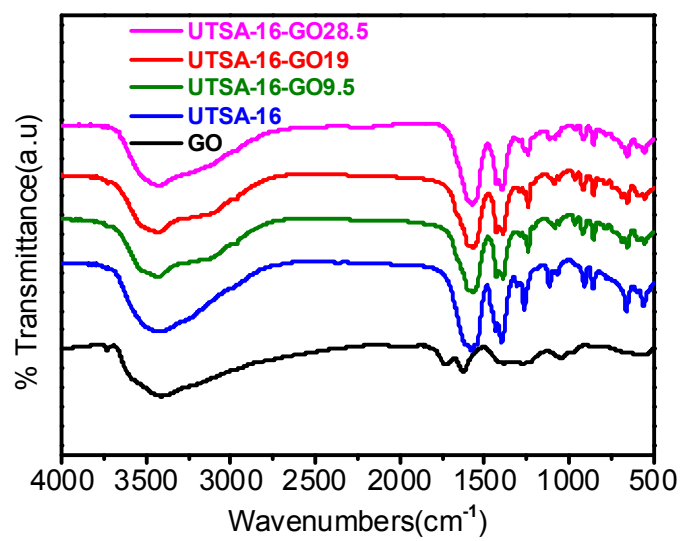


Figure S1 | FTIR spectra of as-synthesized GO, UTSA-16 and composites.

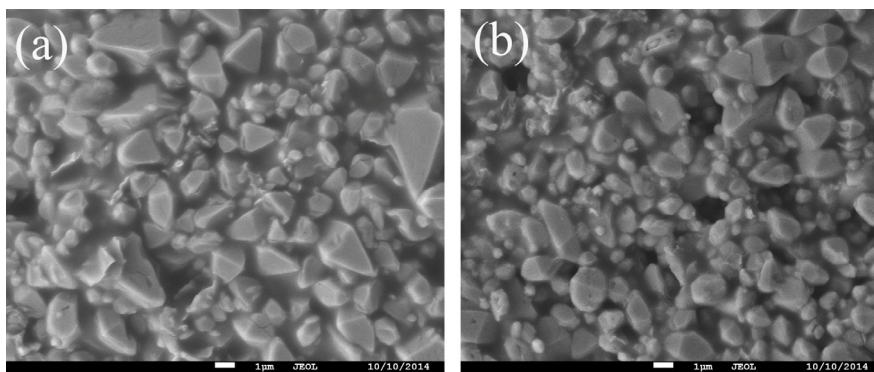


Figure S2 | SEM images for UTSA-16-GO9.5 (a) and UTSA-16-GO28.5 (b).

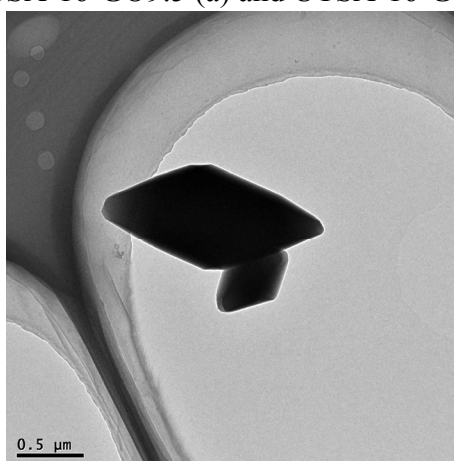


Figure S3 | TEM images for UTSA-16.

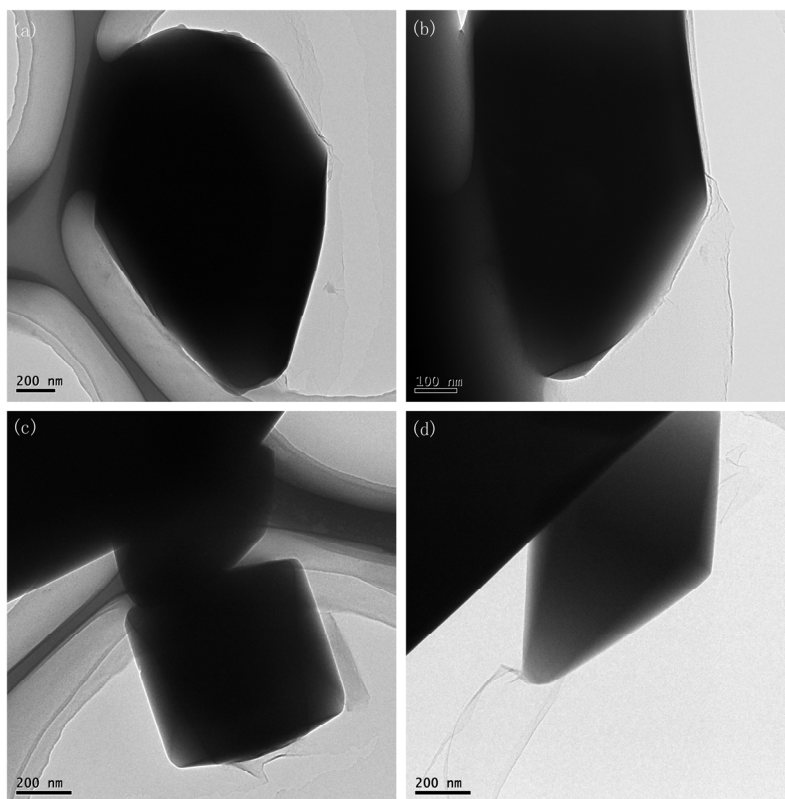


Figure S4 | TEM images for UTSA-16-GO9.5 (a, b), UTSA-16-GO28.5 (c, d).

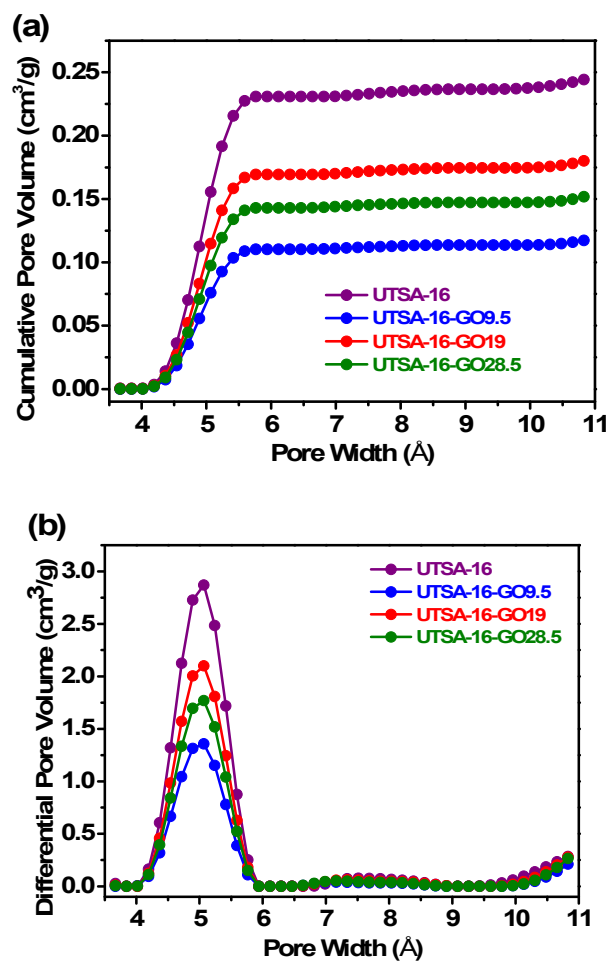


Figure S5 | (a) Cumulative pore volume and (b) pore-size distribution for UTSA-16 and its composites from CO₂ adsorption at 273 K (calculated by using a slit pore NLDFT model).

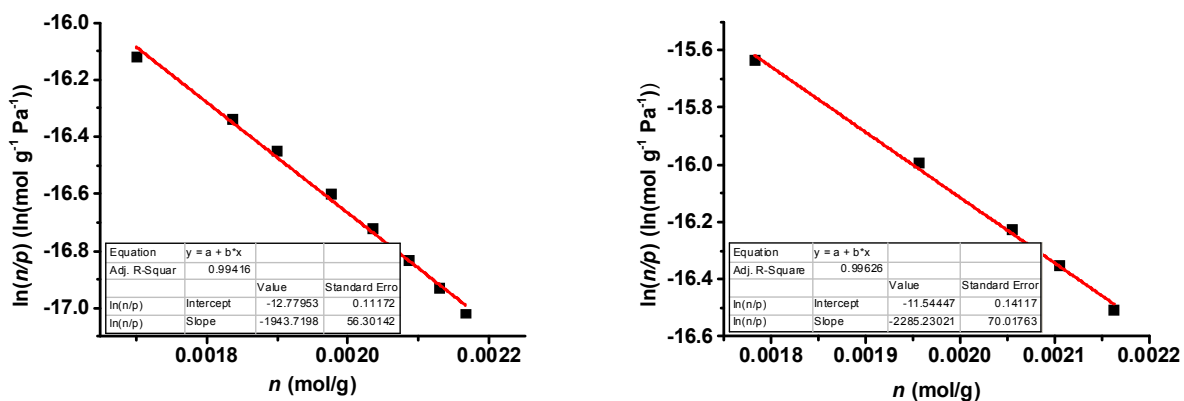


Figure S6 | The virial graphs for adsorption of CO₂ on UTSA-16-GO9.5 at 296 K (left) and 273 K (right).

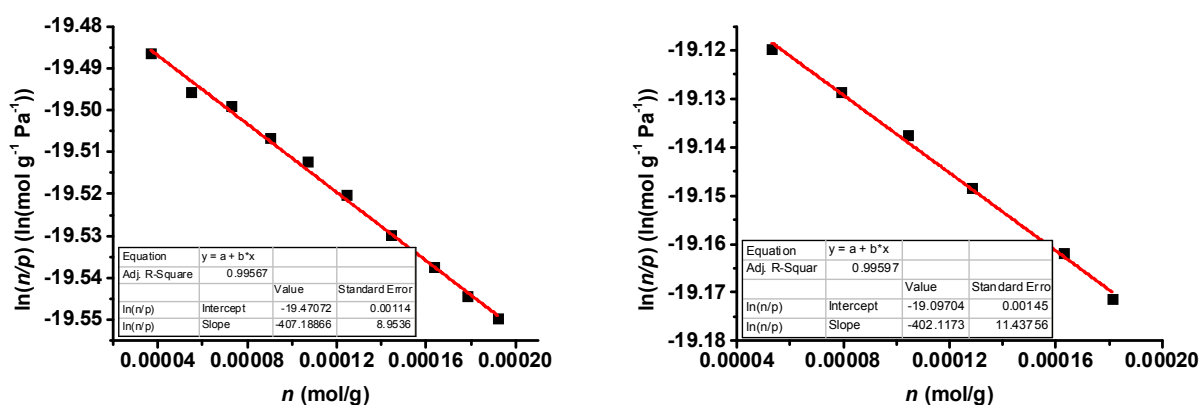


Figure S7 | The virial graphs for adsorption of CH₄ on UTSA-16-GO9.5 at 296 K (left) and 273 K (right).

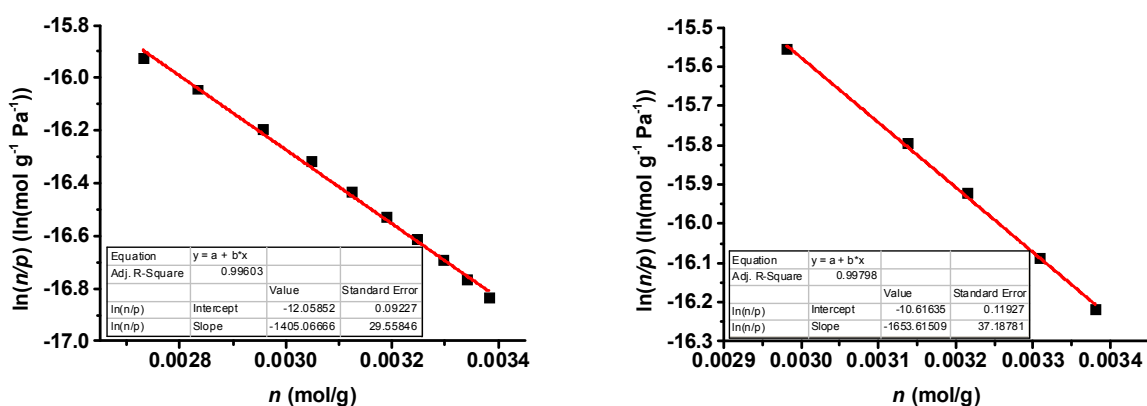


Figure S8 | The virial graphs for adsorption of CO₂ on UTSA-16-GO19 at 296 K (left) and 273 K (right).

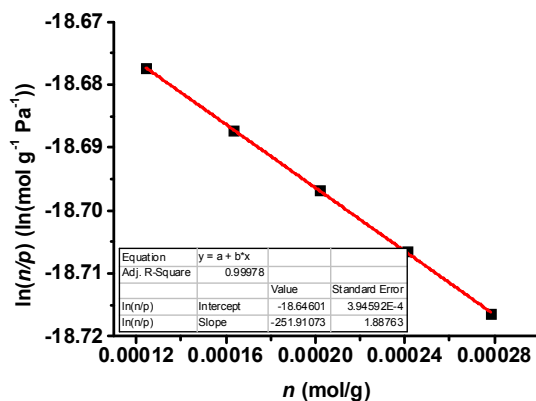
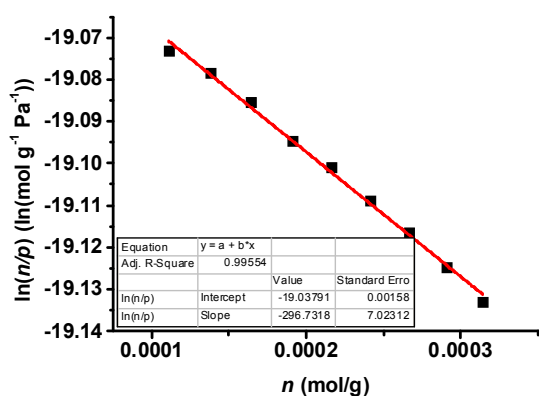


Figure S9 | The virial graphs for adsorption of CH₄ on UTSA-16-GO19 at 296 K (left) and 273 K (right).

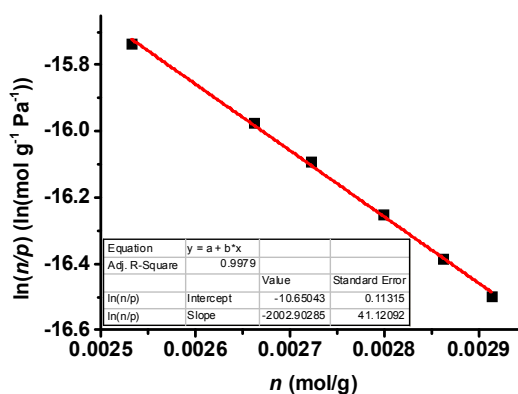
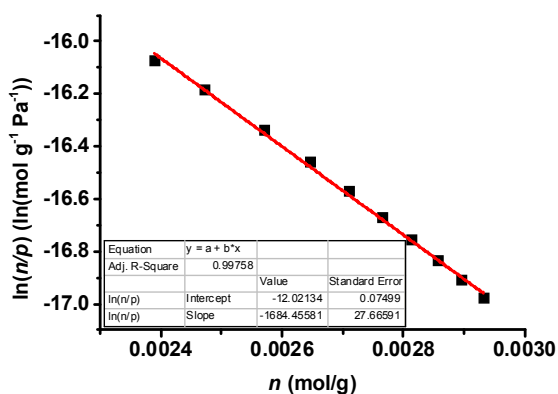


Figure S10 | The virial graphs for adsorption of CO₂ on UTSA-16-GO28.5 at 296 K (left) and 273 K (right).

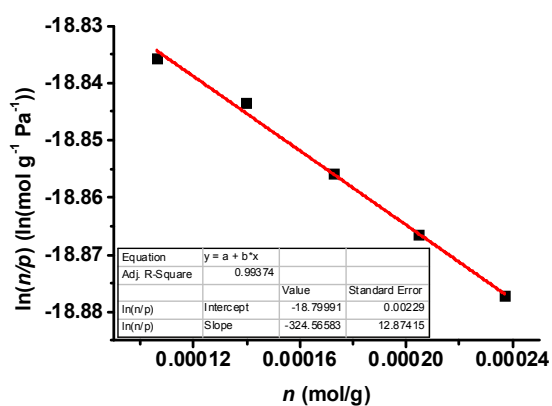
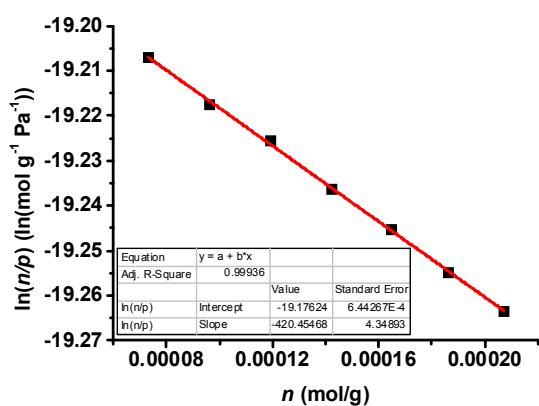


Figure S11 | The virial graphs for adsorption of CH₄ on UTSA-16-GO28.5 at 296 K (left) and 273 K (right).

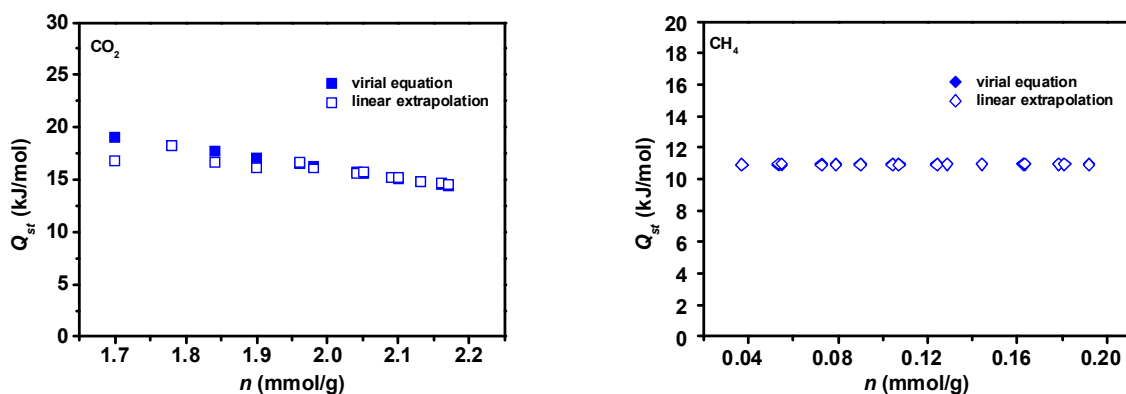


Figure S12 | Comparison of the enthalpies for gas adsorption of CO₂ (left), CH₄ (right) on UTSA-16-GO9.5 from two methods: virial equation (solid) and linear extrapolation (open).

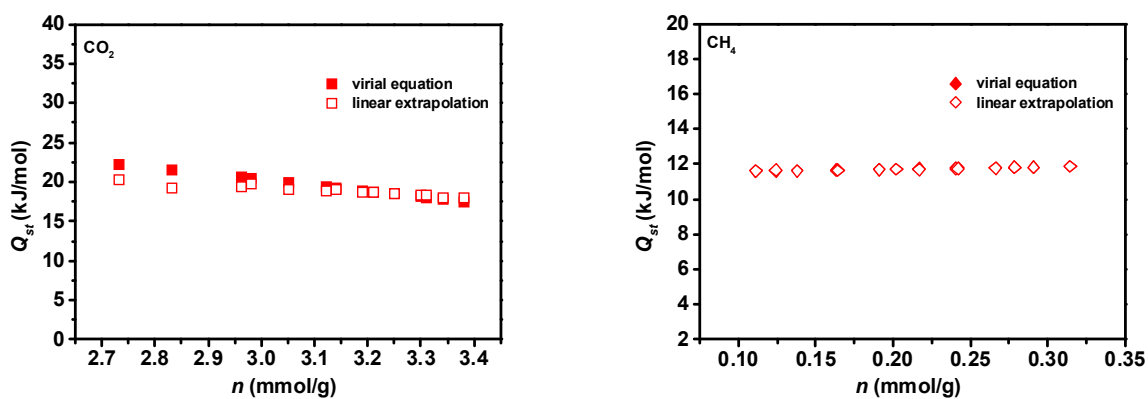


Figure S13 | Comparison of the enthalpies for gas adsorption of CO₂ (left), CH₄ (right) on UTSA-16-GO19 (magenta) from two methods: virial equation (solid) and linear extrapolation (open).

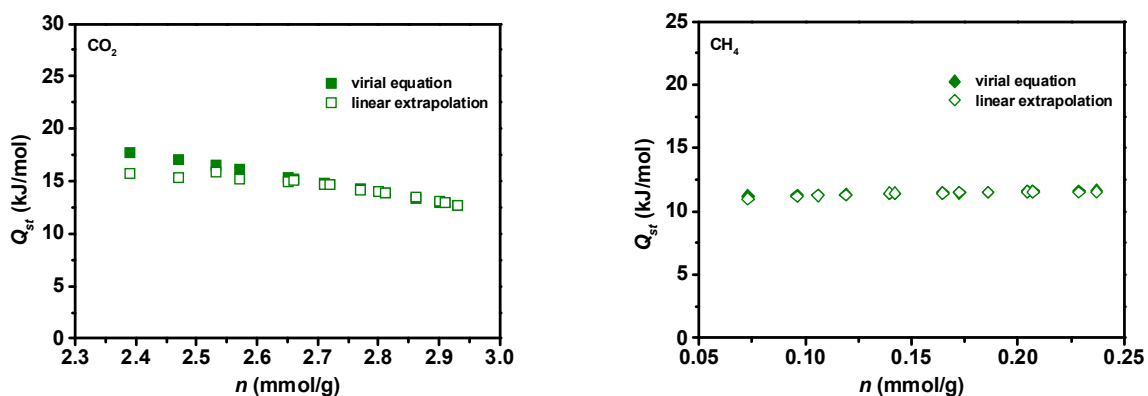


Figure S14 | Comparison of the enthalpies for gas adsorption of CO₂ (left), CH₄ (right) on UTSA-16-GO28.5 (olive) from two methods: virial equation (solid) and linear extrapolation (open).

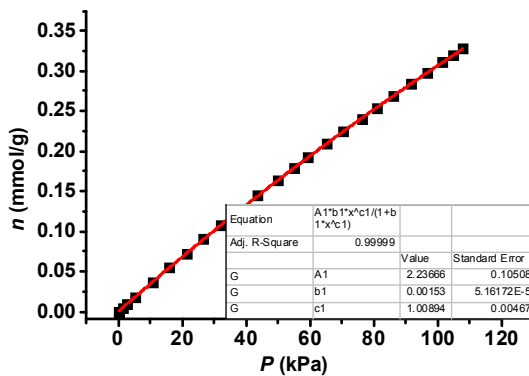
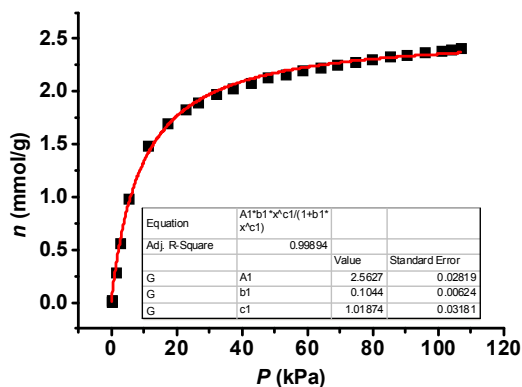


Figure S15 | The graphs of the Single-site Langmuir-Freundlich equations fit for adsorption of CO₂ (left) and CH₄ (right) on UTSA-16-GO9.5 at 296K.

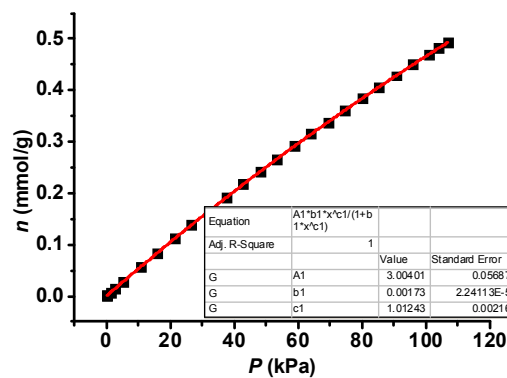
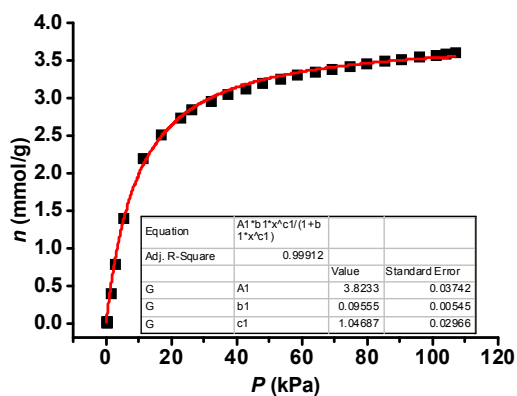


Figure S16 | The graphs of the Single-site Langmuir-Freundlich equations fit for adsorption of CO₂ (left) and CH₄ (right) on UTSA-16-GO19 at 296K.

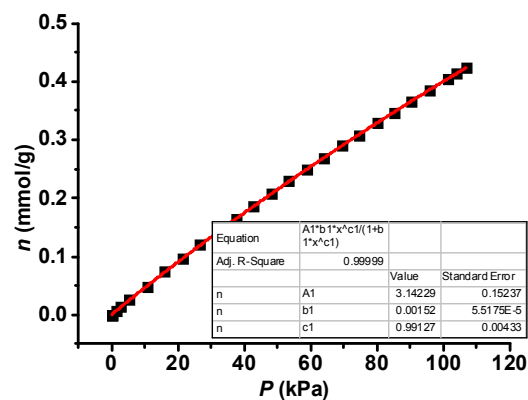
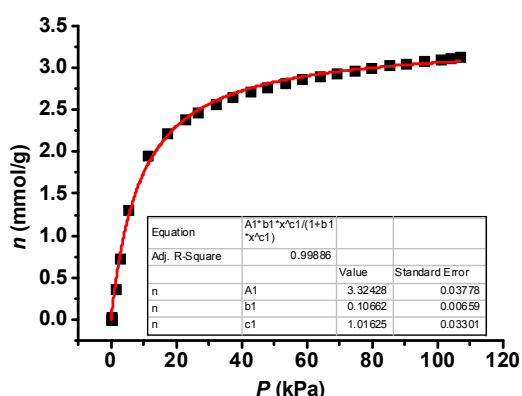


Figure S17 | The graphs of the Single-site Langmuir-Freundlich equations fit for adsorption of CO₂ (left) and CH₄ (right) on UTSA-16-GO28.5 at 296K.

Supplementary References

- (1) Q. Yan, Y. Lin, C. Kong and L. Chen, *Chem. Commun.*, 2013, **49**, 6 873.
- (2) S. -C. Xiang, Y. -B. He, Z. -J. Zhang, H. Wu, W. Zhou, R. Krishna and B. -L. Chen, *Nature Commun.*, 2012, **3**, 954.
- (3) L. Hou, W. -J. Shi, Y. -Y. Wang, Y. Guo, C. Jin and Q. -Z. Shi, *Chem. Commun.*, 2011, **47**, 5464.
- (4) W. Lou, J. Yang, L. Li and J. Li. *J. Solid State Chem.*, 2014, **213**, 224.
- (5) Q. Yang, A. D. Wiersum, P. L. Llewellyn, V. Guillermin, C. Serre and G. Maurin, *Chem. Commun.*, 2011, **47**, 9603.
- (6) D. Saha, Z. Bao, F. Jia and S. Deng, *Environ. Sci. Technol.*, 2010, **44**, 1820.
- (7) E. Atci, I. Erucar and S. Keskin, *J. Phys. Chem. C*, 2011, **115**, 6833.
- (8) S. D. Burd, S. Ma, J. A. Perman, B. J. Sikora, R. Q. Snurr, P. K. Thallapally, J. Tian, L. Wojtas and M. J. Zaworotko, *J. Am. Chem. Soc.*, 2012, **134**, 3663.
- (9) P. Chowdhury, S. Mekala, F. Dreisbach and S. Gumma, *Microporous Mesoporous Mater.*, 2012, **152**, 246.
- (10) H. Alawisi, B. Li, Y. He, H. D. Arman, A. M. Asiri, H. Wang and B. Chen, *Cryst. Growth Des.*, 2014, **14**, 2522.
- (11) V. Finsy, L. Ma, L. Alaerts, D. E. D. Vos, G. V. Baron and J. F. M. Denayer, *Microporous Mesoporous Mater.*, 2009, **120**, 221.